University of Reading

Synergetic effect of carbon nanopore size and surface oxidation on CO2 capture from CO2/CH4 mixtures

Article

Accepted Version

Furmaniak, S., Kowalczyk, P., Terzyk, A. P., Gauden, P. A. and Harris, P. J. F. (2013) Synergetic effect of carbon nanopore size and surface oxidation on CO2 capture from CO2/CH4 mixtures. Journal of Colloid and Interface Science, 397. pp. 144-153. ISSN 0021-9797 doi: 10.1016/j.jcis.2013.01.044
Available at https://centaur.reading.ac.uk/31729/

It is advisable to refer to the publisher's version if you intend to cite from the work. See Guidance on citing.
Published version at: http://dx.doi.org/10.1016/j.jcis.2013.01.044
To link to this article DOI: http://dx.doi.org/10.1016/j.jcis.2013.01.044

Publisher: Elsevier

All outputs in CentAUR are protected by Intellectual Property Rights law, including copyright law. Copyright and IPR is retained by the creators or other copyright holders. Terms and conditions for use of this material are defined in the End User Agreement.

www.reading.ac.uk/centaur

University of Reading

CentAUR

Central Archive at the University of Reading

Reading's research outputs online

Synergetic effect of carbon nanopore size and surface oxidation on carbon dioxide capture from its mixtures with methane

Sylwester Furmaniak[*,1], Piotr Kowalczyk[2], Artur P. Terzyk[1], Piotr A. Gauden[1], and Peter J.F. Harris[3]

[1] Department of Chemistry, Physicochemistry of Carbon Materials Research Group, N. Copernicus University, Gagarin St. 7, 87-100 Toruń, Poland

[2] Nanochemistry Research Institute, Department of Chemistry, Curtin University of Technology, P.O. Box U1987, Perth, 6845 Western Australia, Australia

[3] Centre for Advanced Microscopy, University of Reading, Whiteknights, Reading RG6 6AF, UK

Corresponding author footnote (*To whom correspondence should be addressed):

dr Sylwester Furmaniak

tel.: +48 (56) 611 44 27

fax: +48 (56) 654 24 77

e-mail: sf@chem.umk.pl

Abstract

We studied the synergetic effect of confinement (carbon nanopore size) and surface chemistry (the number of carbonyl groups) on carbon dioxide capture from its mixtures with methane at operating conditions of industrial adsorptive separation. Although both confinement and surface oxidation impacts on the efficiency of carbon dioxide/methane adsorptive separation at thermodynamics equilibrium, we showed that rarely studied surface functionalization is far more important for the designing of an efficient adsorbent for carbon dioxide capture. Systematic Monte Carlo simulations revealed that adsorption of methane either pure or mixed with carbon dioxide on oxidized nanoporous carbons is only slightly increased by the presence of charged functional groups. In contrast, adsorption of carbon dioxide is very sensitive to the number of carbonyl groups (charged dipoles), which can be examined by a strong electric quadrupolar moment of carbon dioxide. Interestingly, the adsorbed amount of methane is strongly affected by the presence of the co-adsorbed carbon dioxide. In contrast, the carbon dioxide uptake does not depend on the molar ratio of methane in the bulk mixture. The optimal carbonaceous porous adsorbent used for carbon dioxide capture near ambient conditions should consist of narrow carbon nanopores and large number of oxygen-containing functional groups dispersed on the carbon pore walls. Furthermore, the carbon dioxide/methane mixtures with dilute carbon dioxide component maximized the equilibrium separation factor. The maximum equilibrium selectivity of CO_2 over CH_4 of ~18-20 is theoretically predicted for strongly oxidized nanoporous carbons. Our interesting findings call for a review of the standard uncharged model of carbonaceous materials used for the modeling of the real adsorption separation processes of gas mixtures containing carbon dioxide (and other molecules with strong electric quadrupolar moment or dipole moment).

Key words: carbon dioxide capture, adsorptive separation, oxidized carbonaceous materials, molecular simulations, and coalbed methane recovery

1. Introduction

The study of adsorption and separation of CO_2-CH_4 mixtures on pure and oxidized nanoporous carbonaceous materials near ambient operating conditions is important from both fundamental and practical perspectives. From fundamental perspective: the equilibrium adsorption and separation of molecules with large electric quadrupolar moment like CO_2 depends on two factors: the size/topology of carbon nanopores (i.e., effect of nanoscale confinement), and the specific short-range interactions with oxygen-containing functional groups dispersed on the carbon surface.[1-15] It is expected that specific dipole-quadrupolar interactions give rise to preferential adsorption of CO_2 over non- and weakly polar fluids (e.g. CH_4, N_2, SF_6, H_2, C_2H_5, C_2H_4, and others) at low pore loadings.[13,14,16-28] Furthermore, it is commonly known that enhanced adsorption field in carbon nanopores increases CO_2 adsorption capacity and the equilibrium separation factor over mentioned above fluids at low pore loadings.[5-10,15,29-35] However, it is not clear how various factors, including: bulk mixture composition, pore loading, the number and type of surface oxygen-containing groups, and carbon texture impact on the CO_2/CH_4 separation factor near ambient operating conditions. From practical perspective: developing methods to energy efficient capture of CO_2 from industrial combustion exhaust gases is a challenge with enormous environmental implications. Optimization of CO_2/CH_4 separation factor is also crucial for practical implementation of novel solutions in clean energy technologies, such as: coalbed methane recovery, geologic CO_2 sequestration, shale gas exploration, and others.[15,36-42]

Oxygen is chemically bounded to the carbon surface in the course of oxidation.[43-47] Unsaturated carbon edge faces are oxidized by exposure to air at room temperature. This

phenomenon, called "aging", depends on the relative humidity, temperature, and the reactivity/topology of carbonaceous material. Therefore, no pure carbonaceous material exists, but carbon surface becomes more and more oxidized (i.e., hydrophilic) with the time. It is to be expected that most of oxygen is bounded by covalent bounds in the form of oxygen-containing functional groups, such as: carboxyl, phenolic hydroxyl, carbonyl, carboxylic anhydrides, lactones, lactols, and ether-type oxygen atoms.[43-45,48,49] Obviously, one can easily adjust the number and chemistry of the oxygen-containing functional groups on carbon surface by controlled oxidation processes. Concentrated nitric acid, perhydrol, and potassium permanganate are most common oxidation agents.[45,48,50-53] Because, overall, oxidation transforms hydrophobic carbon surface to more hydrophilic one, adsorption of organics from aqueous solutions strongly depends on the number and types of oxygen-containing functional groups. Water clusters bounded to the oxidized pore entrances reduce the pore accessibility for organics.[54-57] It has also been shown that the number and types of oxygen-containing functional groups strongly affect adsorption of water vapor, especially at low humidity.[58-63] The mechanism of water adsorption involves the nucleation of water clusters on the acidic functional groups, and further fusion of these clusters at higher humidity.[64-67] Similarly to water adsorption, acidic surface oxides increase the adsorption capacity for other polar molecules such as ammonia and alcohols vapors.[68-72]

In contrast, the impact of oxidation on the adsorption and separation of non- and weakly polar fluids from the gas phase is poorly understood. Tamon and Okazaki[72] investigated the influence of acidic surface oxides of activated carbon on gas adsorption characteristics. The authors showed that mild oxidation of microporous CAL activated carbon sample by HNO_3 slightly reduces micropore volume and surface area. Thus, the oxidation of micro- and nanoporous carbonaceous materials by exposure to air at room temperature is not expected to impact on the surface topology and porosity of carbonaceous materials. As others,

Tamon and Okazaki[72] found that during adsorption of water and ammonia from the gas phase, adsorption capacity increases greatly with oxidation of carbon sample. Furthermore, ammonia was irreversibly adsorbed on the oxidized carbon samples. In constant, the adsorption isotherms of simple alcohols (i.e., CH_3OH, C_2H_5OH, and others), C_6H_6, and C_6H_{12} on pure and oxidized carbon samples were almost identical. Thus this experiment shows that the presence of the specific short-range interactions between some polar molecules and oxygen-containing functional groups not necessary increases their adsorption. Cluster formation around oxygen-containing functional groups is a possible explanation of these experimental findings. In contrast to water, the clustering of other polar molecules around charged O-C dipole is expected to be much weaker. First, these polar molecules are larger than water. The packing at restricted nanospaces may inhibit the accessibility of functional group to clusters composed of larger polar molecules. Second, the strength of hydrogen bonds (H-bonds) formed by other polar molecules is much weaker as compared to water. Because the clusters of polar molecules are too small, they do not aggregate at higher vapor pressures. Thus, the adsorbed amount is not enhanced by the cluster-mediated mechanism of adsorption that is responsible for high water uptake. What about adsorption of CO_2 on pure and oxidized carbonaceous materials? From the electronic properties, it is expected that large electric quadrupolar moment of CO_2 (i.e., 13.4×10^{-40} C/m^2), will develop the specific short-range directional interactions with the charged oxygen-containing functional groups.[13,14,16-28] Therefore at low pore loadings, the equilibrium CO_2/CH_4 separation factor should increase with the content of the charged surface oxygen. However two important questions arises. First, how much the CO_2/CH_4 separation efficiency will increase with the surface oxidation? Second, how the CO_2/CH_4 separation efficiency on pure and oxidized carbonaceous materials depends on the pore size and bulk/pore mixture composition?

In contrast to surface chemistry, the impact of the pore size on the adsorption and separation of CO_2 from the gas mixtures by nanoporous carbonaceous materials has been explored and understood. Recently, Sevilla and Fuertes[73] have summarized the CO_2 adsorption capacities for various carbonaceous materials measured at 298 K and 1 bar. As expected, CO_2 adsorption capacity is strongly correlated with the content of narrow carbon nano- and micropores. Activated graphite fibers and mesoporous carbons adsorb only 1.3-1.7 mmol/g (storage per mass: 59-76 mg/g). In contrast, highly microporous sustainable porous carbon samples prepared by chemical activation of hydrothermally carbonized polysaccharides and biomass are able to adsorb 5.5-5.8 mmol/g (storage per mass: 230-256 mg/g). Furthermore, these porous carbons exhibit a high CO_2 adsorption rate, a good selectivity for CO_2-N_2 separation and can be easily prepared. Silvestre-Albero *et al.*[74] reported similar high CO_2 adsorption uptake in microporous carbon samples produced by the chemical activation of petroleum pitch (i.e., 4.7 mmol/g, storage per mass: 207 mmol/g at 293 K and 1 bar). Finally, Builes *et al.*[75] investigated the CO_2 uptake in two samples of novel microporous zeolite template carbons (i.e., EMT-ZTC and FAU-ZTC). Both carbon samples adsorbed exceptionally high amount of CO_2 at higher pressures, ~30-35 mmol/g at 273 K and 30 bar. It is worth to point out that these CO_2 adsorption capacities are competitive to the best organic and inorganic adsorbing frameworks (zeolites and mesoporous silicas, COFs and MOFs). Taking into account experimental and recent theoretical results obtained by Palmer *et al.*[10] and Kowalczyk *et al.*[76], it seems reasonable to assume that carbonaceous materials with a large number of narrow carbon nanopores (pore size ~ 0.5-0.6 nm) are optimal for CO_2 adsorption. In strong confinement imposed by carbon nanopores, the linear shaped CO_2 molecules have broken rotational symmetry. Highly oriented adsorbed CO_2 molecules maximized their dispersion interactions with carbon pore walls. Moreover, as has been also shown, the equilibrium separation factor of CO_2 over other simple molecules is also very high

in narrow carbon nanopores.[6,29] Nevertheless, we need to take care to the conclusions that have been taken from experimental results. This is because the experimental samples of carbonaceous materials are never pure carbon. They inherently poses some surface functional groups, defect, heteroatoms, mineral contaminants, etc. Therefore it is hard or even impossible to isolate the impact of porosity and surface oxidation on the CO_2 adsorption and separation from the raw experimental measurements. Computer simulation studies are powerful methods that complement and extrapolate experimental knowledge.

In the current work we study the cooperative effect of the structural heterogeneity (i.e., distribution of nanopore sizes) and surface oxidation on the equilibrium CO_2/CH_4 mixture adsorption and separation at 298 K. For this purpose we systematically investigated the CO_2/CH_4 single-component and mixture adsorption on a series of the well-defined pure/oxidized virtual porous carbon samples (VPCs) at various operating conditions, including the entire range of CO_2 molar fractions in the bulk mixture. Most of the experimental work in the literature focuses on the either the impact of the porosity or the surface chemistry on the CO_2 capture by adsorption. On the other hand, the simulation studies have been limited to pure carbonaceous materials that are poor approximation to these used in industrial separation processes. Therefore, in the current work we concentrated on two major issues. First, we used Monte Carlo simulations to advance our understanding at the microscopic level of the adsorption mechanism of CO_2/CH_4 mixtures on pure/oxidized carbonaceous materials at industrial operating conditions. Second, we predicted theoretically the maximum equilibrium selectivity of CO_2 over CH_4 on pure/oxidized carbonaceous materials at 298 K. We believe that presented results are not limited to carbonaceous materials and they are viable information for designing of efficient adsorbents for the equilibrium CO_2/CH_4 mixture separation.

2. Calculation details

2.1. Simulation boxes

The S00 virtual porous carbon (VPC) sample proposed by Harris *et al.*[77-83] was used to generate a sequence of VCPs samples with different porosity. This sequence was obtained by random placing of subsequent small carbon fragments to pores of the S00 VPC sample.[83] Therefore, the pore size distributions of generated VPSs were progressively shifted to narrower carbon nanopores. Subsequent VPCs samples were denoted respectively as S00, S04, S08, S12, S16, S20, S24, S28, S32, and S35 (where the number denotes the number of introduced carbon fragments). Additionally, two representative samples of VPCs (i.e., S00 and S35) were *virtually oxidized*[13] in order to study the impact of the surface oxidation (more precisely, the number of carbonyl groups) on the CO_2/CH_4 mixture separation. Note that the S35 sample contains the narrower carbon nanopores, whereas the S00 sample contains the wider ones. The following VPCs samples were generated from *virtual oxidation* of S00 sample: S00_036, S00_072, S00_108, S00_144, and S00_180.[13] Here, the second number denotes the number of introduced carbonyl groups. Similarly, the following VPCs samples were generated from *virtual oxidation* of S35 sample: S35_072, S35_144, S35_216, S35_288, and S35_360.[14] All carbonaceous samples were placed in a cubicoid simulation box having dimensions 4.6 × 4.6 × 4.6 nm with periodic boundary conditions in x, y, and z direction, as is presented in Figure 1.

The porosity of VPCs samples was evaluated from the geometrical method of Bhattacharya and Gubbins (BG).[84] Following to BG method, the uniform grid of points was generated in the simulation box (here we used 100×100×100). Next, for each such point (located in a pore) the largest sphere containing this point (and situated in the pore) was found and recorded. Its diameter corresponds to the pore size. From the statistical analysis of data

for all points we determined the histograms of pore diameters for all studied VPCs samples (see References 13 and 85 for details).

2.2. Monte Carlo simulations

We used grand canonical Monte Carlo method (GCMC) to study the equilibrium CO_2/CH_4 mixture adsorption/separation at 298 K.[86-88] We investigated four values of the total CO_2/CH_4 mixture pressure. Because of industrial interests, we selected the atmospheric pressure (0.1 MPa) and three higher pressures, i.e. 0.25, 0.5, and 1.0 MPa. For each total pressure we studied the following CO_2 mole fractions in bulk phase (y_{CO2}): 0.0, 0.01, 0.025, 0.05, 0.1, 0.2, 0.3, 0.4, 0.5, 0.6, 0.7, 0.8, 0.9, 0.95, 0.975, 0.99 and 1.0. In our GCMC simulations, the previous configuration of adsorbed mixture was updated by the randomly selected perturbation: (i) displacement and/or rotation of randomly chosen molecule, (ii) creation of new molecule, (iii) annihilation of randomly chosen existing molecule or (iv) swap move with equal probabilities. We used equal probability for each perturbation to guarantee the condition of microscopic reversibility. Each GCMC simulation run consisted of 2.5×10^8 iterations. The first 1.0×10^8 iterations were discarded to guarantee equilibration.

As previously, we used the rigid model for both CO_2 and CH_4 molecules.[13-15,76,89-92] The three-site model with force field developed by Nguyen was used for CO_2.[93] For CH_4 we used revised five-site model proposed by Sun *et al*.[89] The values of the parameters for the carbonaceous skeleton and the atoms forming carbonyl groups were taken from our previous studies.[13,14,59,90] Table 1 collects all applied values of the interaction parameters. The Lorentz–Berthelot mixing rules were used calculation of cross-term energy parameters. Other computations details are documented in our previous works, in details.[13,14,89,90]

From GCMC simulations, we determined the average numbers of CO_2 and CH_4 in the simulation box (i.e., $\langle CO_2 \rangle$ and $\langle CH_4 \rangle$). Than the mole fraction of CO_2 and CH_4 in the adsorbed phase is simply given by:

$$x_{CO_2} = \frac{\langle CO_2 \rangle}{\langle CO_2 \rangle + \langle CH_4 \rangle} \quad (1)$$

$$x_{CH_4} = \frac{\langle CH_4 \rangle}{\langle CO_2 \rangle + \langle CH_4 \rangle} \quad (2)$$

The equilibrium selectivity of CO_2 over CH_4 is computed from well-known relation[87]

$$S_{CO_2/CH_4} = \frac{x_{CO_2} / x_{CH_4}}{y_{CO_2} / y_{CH_4}} \quad (3)$$

where x and y are the mole fractions of the studied mixture components in adsorbed and bulk phase, respectively. The enrichment of adsorbed phase in CO_2 mixture component corresponds to $S_{CO_2/CH_4} > 1$.

3. Results and discussion

Knowledge of the pore size distribution of carbonaceous materials is one the most important factor that impact on the efficiency of the adsorptive separation. Figure 2 shows the histograms of pore diameters computed for studied pure VPCs (samples: S00-S35). Taking into account the International Union of Pure and Applied Chemistry (IUPAC) classification of pores, all studied VPCs are microporous materials (i.e., pore diameters are less than 2 nm).

Passing from S00 to S35 sample, we notice a gradual increasing from the contribution of the smallest carbon nanopores. Further, as we added more and more carbon fragments to S00 VPC sample, the pore size distributions are more homogenous and shifted to smaller carbon nanopores. Figures S1 and S2 attached to supporting information display the histograms of pore diameters for studied samples of oxidized VPCs. The most important conclusion is that *virtual oxidation* of VPCs does not affect the porosity of pure carbonaceous samples (i.e., carbon templates used for oxidation). This observation is in good agreement with the experiment, which further confirms the realism of the *virtual oxidation* algorithm.

Figures S3-S5 attached to supporting information depict CO_2 and CH_4 single-component adsorption isotherms computed from GCMC for all studied VPCs samples. Here we expressed the absolute value of adsorption as an average number of molecules in the simulation box. For comparison and further discussion of simulation results, we expressed the absolute value of adsorption as an average number of molecules per unit mass adsorbent too. As would be expected, both porosity and oxygen content affect the adsorption of both CO_2 and CH_4 adsorbates. Interestingly, regardless the porosity and oxidation intensity of studied VPCs, the CO_2 adsorption amount is at least two times greater than the CH_4 adsorption amount. Further, we notice that for both CO_2 and CH_4 narrowing of pore diameters results in higher number of adsorbed molecules in the simulation box. Region of high pressures is an exception. This is because the nanopore volume accessible for adsorbed molecules is decreasing by adding additional graphitic fragments to the initial S00 VPC sample (see upper panel in Figure S3 attached to supporting information). As would be expected, the CO_2 and CH_4 adsorbed amount expressed per unit mass of adsorbent is decreasing with the narrowing of the pore diameters. A significant increase in the number of carbon atoms in the simulation box for VPCs samples characterized by the narrow nanoporosity is responsible for this effect (compare sample S00 and S35). Careful inspection of simulation results revealed that the

single-component CO_2 adsorption isotherms are more affected by the porosity/surface oxidation than the single-component CH_4 ones. The increase in the oxygen content causes an increase in adsorption of both studied adsorbates. However, we notice that the presence of carbonyl functional groups affects the CO_2 uptake far more than CH_4 one (see Figures S4 and S5 attached to supporting information). In the case of CH_4, the presence of oxygen-containing groups increases slightly the adsorption, while the CO_2 uptake is increased by up to several tens of percent. Analogical effects were reported in our previous papers.[13,14,90] Observed regularities can be easily explained by the electric nature of studied adsorbates. CO_2 molecule has strong electric quadrupolar moment, while CH_4 has only weak electric octupolar moment. Therefore, the electrostatic interactions of CO_2 with carbonyl groups (which are dipoles) are far stronger and slowly decrease with the intermolecular distance in the comparison with CH_4.[94]

For clarity of the presented simulation results, for all studied CO_2/CH_4 mixtures, we expressed the adsorption amount of mixture components as an average number of molecules in the simulation box. Clearly, one should expect that the electrostatic interactions pay an essential role in a case of CO_2/CH_4 mixture adsorption and separation. However, we need bear in mind that co-adsorption and displacement of mixture components from carbon nanopores is also affected by their mutual interactions (particularly at high pore loadings). Figures 3-5 display the variation of the CO_2 mole fraction and equilibrium selectivity as a function of the CO_2 mole fraction in the bulk mixture. Additionally, Figures S6-S8 attached to supporting information present the comparison between the average number of CO_2 and CH_4 molecules in simulation boxes. We notice that for all studied VPCs samples the CO_2 mole fraction in the adsorbed phase (x_{CO2}) is significantly higher than in the gaseous phase (y_{CO2}). This is because CO_2 molecules are preferentially adsorbed over CH_4 ones. Furthermore, the equilibrium selectivity is monotonically decreasing with the concentration of CO_2 in the bulk

mixture. This monotonic reduction in the equilibrium separation factor is strongly marked for low and moderate CO_2/CH_4 total mixture pressures. Here, we predicted that CO_2/CH_4 mixtures with dilute CO_2 mixture component can be efficiently separated by studied VPCs materials. Interestingly, for high total CO_2/CH_4 mixture pressures, we predicted a non-monotonic variation of the equilibrium selectivity with the CO_2 concentration in the bulk mixture. Here, equilibrium selectivity is higher for high CO_2 concentration in the bulk mixture as compared to its infinite dilution. Therefore we suggest that the CO_2/CH_4 mixtures can be also efficiently purified by adsorption at high operating pressures. The energy consumption of high-pressure adsorptive separation favors the CO_2/CH_4 mixtures with low CO_2 concentration.

Let us now analyze the CO_2/CH_4 mixture adsorption on pure VPCs in details (i.e., S00-S35, see Figure 3). Regardless the total pressure and mixture composition, CO_2 mole fraction increases with narrowing of the pore diameters (i.e., from S00 sample to S35 one). That is why we observe an enhancement of the equilibrium selectivity by 1-2 for VPCs samples consisting the significant fraction of narrow carbon nanopores. Interestingly, the strongest effect is observed for the total CO_2/CH_4 mixture pressure of 1 MPa. Here, for all VPCs samples, the variation of equilibrium selectivity with the CO_2 concentration in the bulk mixture is non-monotonic, with initial decreasing and further increasing with CO_2 mole fraction in the bulk phase. Similar behavior (but weakly marked) is also observed for lower total pressure in the case of more nanoporous VPCs. This interesting result can be explained by the displacement of CH_4 from nanopores by co-adsorbed CO_2 molecules. As we have shown recently, the displacement of CH_4 from adsorbed phase by co-adsorbed CO_2 is facilitated in narrow carbon nanopores.[15]

The presence of surface functionalities (i.e., oxygen-containing functional groups) has far more important effect on the equilibrium CO_2/CH_4 separation factor comparing to porosity

(see Figures 4 and 5). Increasing of the oxygen content on VPCs results in substantial enhancement of the CO_2 mole fraction in the adsorbed phase. Therefore, the most oxidized VPCs samples (i.e., S00_180 and S35_360) show the equilibrium selectivity of 2-3 times greater than the pure VPCs ones. In the case of the S00_180 structure (having carbon nanopores dispersed in the range up to 2 nm) the equilibrium selectivities approach 8-10, while in the case of strictly nanoporous S35_360 VPC sample (having carbon nanopores with pore diameters below 1 nm) the values of equilibrium selectivities are ~2 times greater. This is a clear manifestation of the synergistic effect of the porosity and the surface oxidation on the energetic of CO_2 adsorption (see Figure 6). As previously, at high total CO_2-CH_2 mixture pressures, we found higher equilibrium separation factor as compared to CO_2 infinite dilution. This is a consequence of CH_4 displacement from carbon nanopores, and the co-adsorption of the CO_2 in the whole accessible pore volume. The comparison between the number of CO_2 molecules adsorbed in pure and oxidized VPCs samples clearly show that oxidized carbonaceous materials adsorb more CO_2 at the same operating conditions (see Figure 6 and Figure S6-S8 attached to supporting information). In contract, for CH_4, the number of adsorbed molecules is only slightly affected by the presence of the carbonyl groups.

Figures 7 and 8 depict the partial pressure variation in the average number of adsorbed CO_2 and CH_4 molecules for selected samples of VPCs. Adsorption data computed for pure mixture components are also presented. We grouped all simulation results in series corresponding to different values of total CO_2/CH_4 mixture pressure. It is clear that the presence of CH_4 practically does not influence CO_2 adsorption from CO_2-CH_4 mixtures. What is more important, this conclusion seems to be correct for different mole fractions of CH_4 in the bulk phase. On the other hand, the presence of CO_2 in the bulk phase (even at low concentrations) strongly affects CH_4 adsorption. Note, that this interesting observation is predicted for both pure and oxidized VPCs samples. If fact, it has been shown experimentally,

that to maximize the CO_2/X equilibrium separation factor (X denotes other component, such as: CH_4, N_2, etc.), one need only to optimize the structure of porous materials in respect to CO_2 adsorption. Our simulation results give deeper understanding of this important feature of adsorptive CO_2/X mixture separation.

Concluding, we showed that CO_2 is preferentially adsorbed over CH_4 on both pure and oxidized VPCs samples. However, the preferential adsorption towards CO_2 is intensified by the decrease in the average pore diameter and by the increase in surface oxidation. Therefore, in order to optimize the performance of activated carbons towards the equilibrium separation of CO_2/CH_4 mixtures its pore size should be decreased and the concentration of oxygen-containing functionalities should be increased. We argue that this conclusion is not limited to CO_2 mixtures with CH_4, but it is more general. Similar trend is expected for adsorptive separation of CO_2-X mixtures (where X is characterized by weaker electrostatic and dispersion interactions with oxidized porous materials as compared to CO_2). Finally, the maximum equilibrium selectivity of CO_2 over CH_4 of ~18-20 is theoretically predicted, which is in good qualitative agreement with experimental results. Finally, we speculate that similar order of CO_2/CH_4 separation factor is expected for other porous materials where the dominant adsorption mechanism is physisorption. Therefore, to further enhance the CO_2/CH_4 separation efficiently the other mechanism of adsorption (such as: partial charge transfer, chemisorption, strong polarization by heavily charged atoms, etc.) needs to be considered.

4. Conclusions

We have presented a detailed study of CO_2/CH_4 mixture adsorption and separation at 298 K on pure and oxidized virtual porous carbons using grand canonical Monte Carlo simulations. To the best of our knowledge, this is the first comprehensive work, where the

synergetic effect of carbon nanopore size and surface oxidation on carbon dioxide adsorptive separation has been described. We found that surface oxidation is far more important factor than carbon nanoporosity that impact on the efficiently of the CO_2/CH_4 mixture separation at thermodynamics equilibrium. This is because short-range electrostatic interactions between adsorbate and charged functional groups are much stronger for carbon dioxide as compared to methane. Therefore both single-component and mixture adsorption of carbon dioxide is significantly enhanced by the presence of charged surface functionalities. Furthermore, we showed that the adsorbed amount of methane is strongly affected by the presence of the co-adsorbed carbon dioxide. Interestingly, carbon dioxide uptake does not depend on the molar ratio of methane in the bulk mixture. Thus, by maximizing of carbon dioxide uptake, one can predict the optimal adsorbent (i.e., its porosity and surface oxidation) as well as operating conditions for its adsorptive separation. As a rule of thumb one can assume that the optimal adsorbent for carbon dioxide capture by equilibrium adsorption mechanism should consist of narrow carbon nanopores decorated by high concentration of charged oxygen-containing functional groups. Moreover, the optimal operating conditions for CO_2/CH_4 mixture separation corresponds to low concentration of carbon dioxide in the bulk mixture. At these operating conditions, the high CO_2/CH_4 equilibrium selectivity results from preferential adsorption of carbon dioxide over methane at the most energetic centers of an adsorbent (i.e., in narrow nanopores with oxidized pore walls). Efficient separation at high CO_2/CH_4 mixture pressures is an interesting option but it will require significant energy consumption. At higher CO_2/CH_4 mixture pressures, the enrichment of adsorbed phase in carbon dioxide component results from displacement of methane from porous adsorbents by co-adsorbed carbon dioxide. High CO_2/CH_4 equilibrium separation factor of ~18-20 at 298 K is theoretically predicted and associated with the strong oxidization of nanoporous carbonaceous materials. Finally, we argue that our conclusions on the efficiently of carbon dioxide capture by adsorption are not

limited to carbonaceous materials, because of the nature of intermolecular forces behind carbon dioxide physisorption. Our simulation results shed some light on the modeling of the adsorption separation processes of gas mixtures containing carbon dioxide on real carbonaceous materials.

Acknowledgments

S.F., A.P.T. and P.A.G. acknowledge the use of the computer cluster at Poznan Supercomputing and Networking Centre (Poznań, Poland) as well as the Information and Communication Technology Centre of the Nicolaus Copernicus University (Toruń, Poland). P.K. acknowledges partial support by the Office of Research & Development, Curtin University of Technology, Grant CRF10084. P. K. acknowledges the use of the iVEC Epic supercomputer. The authors gratefully acknowledge Professor D. N. Theodorou (National Technical University of Athens) for his valuable comments and suggestions.

Supporting Information Available: Histograms of pore diameters for series of oxidized VPCs (Figures S1 and S2), adsorption isotherms of pure components on all studied carbonaceous materials (Figures S3-S5), the comparison of the average number of CO_2 and CH_4 in simulation box for all investigated adsorption systems (Figures S6-S8). This material is available free of charge via the Internet at http://pubs.acs.org.

References

(1) Bansal, R. Ch.; Goyal, M. *Activated Carbon Adsorption*; CRC Press: Boca Rathon, U.S.A., 2005.

(2) Bandosz, T. J. *Activated Carbon Surfaces in Environmental Remediation*; Academic Press: New York, U.S.A, 2006.

(3) Rouquerol, J.; Rouquerol, F.; Sing, K S. W. *Adsorption by Powders and Porous Solids*; Academic Press: London, U.K., 1999.

(4) Moreno-Castilla, C.; Rivera-Utrilla, J.; Carrasco-Marin, F.; Lopez-Ramon, M. V. *Langmuir* **1997**, *13*, 5208-5210.

(5) Cao, D.; Wu, J. *Carbon* **2005**, *43*, 1364-1370.

(6) Cracknell, R. F.; Nicholson, D.; Tennison, S. R.; Bromhead, J. *Adsorption* **1996**, *2*, 193-203.

(7) Heuchel, M.; Davies, G. M.; Buss, E.; Seaton, N. A. *Langmuir* **1999**, *15*, 8695-8705.

(8) Huang, L.; Zhang, L.; Shao, Q.; Lu, L.; Lu, X.; Jiang, S.; Shen, W. *J. Phys. Chem. C* **2007**, *111*, 11912-11920.

(9) Kurniawan, Y.; Bhatia, S. K.; Rudolph, V. *AIChE J.* **2006**, *52*, 957-967.

(10) Palmer, J. C.; Moore, J. D.; Roussel, Th. J.; Brennan, J. K.; Gubbins, K. E. *Phys. Chem. Chem. Phys.* **2011**, *13*, 3985–3996.

(11) Peng, X.; Cao, D.; Zhao, J. *Sep. Purif. Technol.* **2009**, *68*, 50-60.

(12) Peng, X.; Cao, D.; Wang, W. *Ind. Eng. Chem. Res.* **2010**, *49*, 8787-8796.

(13) Furmaniak, S.; Terzyk, A. P.; Gauden, P. A.; Harris, P. J. F.; Kowalczyk, P. *J. Phys.: Condens. Matter* **2009**, *21*, 315005.

(14) Furmaniak, S.; Terzyk, A. P.; Gauden, P. A.; Harris, P. J. F.; Kowalczyk, P. *J. Phys.: Condens. Matter* **2010**, *22*, 085003.

(15) Kowalczyk, P.; Gauden, P. A.; Terzyk, A. P.; Furmaniak, S.; Harris, P. J. F. *J. Phys. Chem. C* **2012**, *116*, 13640-13649.

(16) Walton, K. S.; Millward, A. R.; Dubbeldam, D.; Frost, H.; Low, J. J.; Yaghi, O. M.; Snurr, R. Q. *J. Am. Chem. Soc.* **2008**, *130*, 406-407.

(17) Bae, Y.-S.; Mulfort, K. L.; Frost, H.; Ryan, P.; Punnathanam, S.; Broadbelt, L. J.; Hupp, J. T.; Snurr, R. Q. *Langmuir* **2008**, *24*, 8592-8598.

(18) Bae, Y.-S.; Farha, O. K.; Hupp, J. T.; Snurr, R. Q. *J. Mater. Chem.* **2009**, *19*, 2131-2134.

(19) Liu, Y.; Wilcox, J. *Environ. Sci. Technol.* **2012**, *46*, 1940-1947.

(20) Xu, Q.; Liu, D.; Yang, Q.; Zhong, Ch.; Mi, J. *J. Mater. Chem.* **2010**, *20*, 706–714.

(21) Wu, D.; Xu, Q.; Liu, D.; Zhong, Ch. *J. Phys. Chem. C* **2010**, *114*, 16611-16617.

(22) Liu, D.; Zhong, Ch. *J. Mater. Chem.* **2010**, *20*, 10308-10318.

(23) Choi, Y. J.; Choi, J. H.; Choi, K. M.; Kang, J. K. *J. Mater. Chem. 2011*, **21**, 1073-1078.

(24) Kim, H.; Kim, Y.; Yoon, M.; Lim, S.; Park, S. M.; Seo, G.; Kim, K. *J. Am. Chem. Soc.* **2010**, *132*, 12200-12202.

(25) Zheng, B.; Bai, J.; Duan, J.; Wojtas, L.; Zaworotko, M. J. *J. Am. Chem. Soc.* **2011**, *133*, 748-751.

(26) Park, J. Y.; Lee, Y. S.; Jung, Y. *J. Nanopart. Res.* **2012**, *14*, 793.

(27) Zhang, W.; Huang, H.; Zhong, Ch.; Liu, D. *Phys. Chem. Chem. Phys.* **2012**, *14*, 2317-2325.

(28) Chandra, V.; Yu, S. U.; Kim, S. H.; Yoon, Y. S.; Kim, D. Y.; Kwon, A. H.; Meyyappan, M.; Kim K. S. *Chem. Commun.* **2012**, *48*, 735-737.

(29) Nicholson, D.; Gubbins, K. E. *J. Chem. Phys.* **1996**, *104*, 8126-8134.

(30) Sweatman, M. B. *Adsorption* **2011**, *17*, 723-737.

(31) Wu, J.; Zhou, L.; Sun, Y.; Su, W. *AIChE J.* **2007**, *53*, 1178-1191.

(32) Dreisbach, F.; Staudt, R.; Keller, J. U. *Adsorption* **1999**, *5*, 215-227.

(33) Shao, X.; Feng, Z.; Xue, R.; Ma, C.; Wang, W.; Peng, X.; Cao, D. *AIChE J.* **2011**, *57*, 3042-3051.

(34) Okayama, T.; Yoneya, J.; Nitta, T. *Fluid Phase Equilib.* **1995**, *104*, 305-316.

(35) Fitzgerald, J. E.; Robinson, Jr., R. L.; Gasem, K. A. M. Langmuir **2006**, *22*, 9610-9618.

(36) Lackner, K. S. *Science* **2003**, *13*, 1677-1678.

(37) White, C. M.; Smith, D. H.; Jones, K. L.; Goodman, A. L.; Jikich, S. A.; LaCount, R. B.; DuBose, S. B.; Ozdemir, E.; Morsi, B. I.; Schroeder, K. T. *Energy Fuels* **2005**, *19*, 659-724.

(38) Yu, H.; Zhou, G.; Fan, W.; Ye, J. *Int. J. Coal Geol.* **2007**, *71*, 345-357.

(39) Gale, J.; Freund, P. *Environ. Geosci.* **2001**, *8*, 210-217.

(40) Harpalani, S.; Prusty, B. K.; Dutta, P. *Energy Fuels* **2006**, *20*, 1591-1599.

(41) Prusty, B. K. *J. Nat. Gas Chem.* **2008**, *17*, 29-38.

(42) Mazzotti, M.; Pini, R.; Storti, G. *J. Supercrit. Fluids* **2009**, *47*, 619-627.

(43) Grajek, H.; Świątkowski, A.; Witkiewicz, Z.; Pakuła, M.; Biniak, S. *Adsorpt. Sci. Technol.* **2001**, *19*, 565-576.

(44) Buczek, B.; Biniak, S.; Świątkowski, A. *Fuel* **1999**, *78*, 1443-1448.

(45) Boehm, H.P. *Carbon* **2002**, *40*, 145-149.

(46) Ajayan, P. M.; Yakobson, B. I. *Nature* **2006**, *441*, 818-819.

(47) Carrasco-Marín, F.; Rivera-Utrilla, J.; Joly,, J.-P.; Moreno-Castilla, C. *J . Chem. Soc. Faraday Trans.* **1996**, *92*, 2779-2782.

(48) Marsh, T.H.; Rodríguez-Reinoso, F. *Activated Carbon*; Elsevier: Amsterdam, Holland, 2006.

(49) Biniak, S.; Szymański, G.; Siedlewski, J.; Świątkowski, A. *Carbon* **1997**, *35*, 1799-1810.

(50) Pradhan, B. K.; Sandle, N. K. *Carbon* **1999**, *37*, 1323-1332.

(51) Daifullah, A. A. M.; Yakout, S. M.; Elreefy, S. A. *J. Hazard. Mater.* **2007**, *147*, 633-643.

(52) Moreno-Castilla, C.; Ferro-García, M. A.; Joly, J. P.; Bautista-Toledo, I.; Carrasco-Marín, F.; Rivera-Utrilla, J. *Langmuir* **1995**, *11*, 4386-4392.

(53) Figueiredo, J. L.; Pereira, M. F. R.; Freitas, M. M. A.; Órfão, J. J. M. *Carbon* **1999**, *37*, 1379-1389.

(54) Coughlin, R. W.; Ezra, F. S. *Environ. Sci. Technol. 1968*, *2*, 291-297.

(55) Terzyk, A. P.; Rychlicki, G.; Ćwiertnia, M. S.; Gauden, P. A.; Kowalczyk, P. *Langmuir* **2005**, *21*, 12257-12267.

(56) Terzyk, A. P.; Gauden, P. A.; Furmaniak, S.; Wesołowski, R. P.; Harris, P. J. F. *Phys. Chem. Chem. Phys.* **2010**, *12*, 812-817.

(57) Li, L.; Quinlivan, P. A.; Knappe, D. R.U. *Carbon* **2002**, *40*, 2085-2100.

(58) Furmaniak, S.; Gauden, P. A.; Terzyk, A. P.; Rychlicki, G. *Adv. Colloid Interface Sci.* **2008**, *137*, 82-143.

(59) Jorge, M.; Schumacher, Ch.; Seaton, N. A. *Langmuir* **2002**, *18*, 9296-9306.

(60) Müller, E. A.; Rull, L. F.; Vega, L. F.; Gubbins, K. E. *J. Phys. Chem.* **1996**, *100*, 1189-1196.

(61) Barton, S. S.; Evans, M. J. B.; MacDonald, J. A. F. *Langmuir* **1994**, *10*, 4250-4252.

(62) Barton, S. S.; Evans, M. J. B.; MacDonald, J. A. F. *Carbon* **1996**, *34*, 975-982.

(63) Rutherford, S. W. *Carbon* **2003**, *41*, 622-625.

(64) Do, D. D.; Do, H. D. *Carbon* **2000**, *38*, 767-773.

(65) McCallum, C. L.; Bandosz, T. J.; McGrother, S. C.; Müller, E. A.; Gubbins, K. E. *Langmuir* **1999**, *15*, 533-544.

(66) Brennan, J. K.; Thomson, K. T.; Gubbins, K. E. *Langmuir* **2002**, *18*, 5438-5447.

(67) Ohba, T.; Kaneko, K. *J. Phys. Chem. C* **2007**, *111*, 6207-6214.

(68) Bandosz, T. J.; Jagiełło, J.; Schwarz, J. A. *Langmuir* **1996**, *12*, 6480-6486.

(69) Stoeckli, F.; Guillot, A.; Slasli, A. M. *Carbon* **2004**, *42*, 1619-1624.

(70) Silvestre-Albero, A.; Silvestre-Albero, J.; Sepúlveda-Escribano, A.; Rodríguez-Reinoso, F. *Microporous Mesoporous Mater.* **2009**, *120*, 62-68.

(71) Mangun, Ch. L.; Benak, K. R.; Daley, M. A.; Economy, J. *Chem. Mater.* **1999**, *11*, 3476-3483.

(72) Tamon, H.; Okazaki, M. *Carbon* **1996**, *34*, 741-746.

(73) Sevilla, M.; Fuertes, A. B. *Energy Environ. Sci.* **2011**, *4*, 1765-1771.

(74) Silvestre-Albero, J.; Wahby, A.; Sepúlveda-Escribano, A.; Martínez-Escandell, M.; Kaneko K.; Rodríguez-Reinoso, F. *Chem. Commun.* **2011**, *47*, 6840-6842.

(75) Builes, S.; Roussel, Th.; Ghimbeu, C. M.; Parmentier, J.; Gadiou, R.; Vix-Guterl, C.; Vega, L. F. *Phys. Chem. Chem. Phys.* **2011**, *13*, 16063-16070.

(76) Kowalczyk, P.; Furmaniak, S.; Gauden, P. A.; Terzyk, A. P. *J. Phys. Chem. C* **2010**, *114*, 5126-5133.

(77) Harris, P. J. F.; Tsang, S. C.; *Philos. Mag. A* **1997**, *76*, 667-677.

(78) Harris, P. J. F.; *Int. Mater. Rev.* **1997**, *42*, 206-218.

(79) Harris, P. J. F.; Burian, A.; Duber, S. *Philos. Mag. Lett.* **2000**, *80*, 381-386.

(80) Harris, P. J. F.; Liu, Z.; Suenaga, K. *J. Phys.: Condens. Matt.* **2008**, *20*, 362201.

(81) Harris, P. J. F. In *Carbon Materials – Theory and Practice*; Terzyk, A. P.; Gauden, P. A. Kowalczyk, P., Eds.; Research Signpost: Kerala, India, 2008; pp 1-14.

(82) Harris, P. J. F.; Liu, Z.; Suenaga, K. *J. Phys.: Conf. Ser.* **2010**, *241*, 012050.

(83) Terzyk, A. P.; Furmaniak, S.; Gauden, P. A.; Harris, P. J. F.; Włoch, J.; Kowalczyk, P.; *J. Phys.: Condens. Matt.* **2007**, *19*, 406208.

(84) Bhattacharya, S.; Gubbins, K. E. *Langmuir* **2006**, *22*, 7726-7731.

(85) Furmaniak, S.; Terzyk, A. P.; Gauden, P. A.; Marks, N. A.; Powles, R. C.; Kowalczyk, P. *J. Colloid Interface Sci.* **2011**, *360*, 211-219.

(86) Frenkel, D.; Smit, B. *Understanding molecular simulations*; Academic Press: New York, U.S.A., 2002.

(87) Tylianakis, E.; Froudakis, G.E. *J. Comput. Theor. Nanosci.* **2008**, *6*, 1-14.

(88) Theodorou, D. N. *Ind. Eng. Chem. Res.* **2010**, *49*, 3047-3058.

(89) Terzyk, A. P.; Furmaniak, S.; Gauden, P. A.; Kowalczyk, P. *Adsorpt. Sci. Technol.* **2009**, *27*, 281-296.

(90) Terzyk, A. P.; Furmaniak, S.; Wesołowski, R. P.; Gauden, P. A.; Harris, P. J. F. In *Advances in Adsorption Technology*; Saha, B. B.; Ng, K. C., Eds.; Nova Science Publishers: New York, U.S.A., 2010; ch 14.

(91) Kowalczyk, P.; Furmaniak, S.; Gauden, P. A.; Terzyk, A. P. *J. Phys. Chem. C* **2010**, *114*, 21465-21473.

(92) Kowalczyk, P.; Furmaniak, S.; Gauden, P. A.; Terzyk, A. P. *J. Phys. Chem. C* **2012**, *116*, 1740-1747.

(93) Nguyen, T. X. *Characterization of Nanoporous Carbons*, Ph.D. Thesis; The University of Queensland: Brisbane, Australia, 2006.

(94) Gray, C. G.; Gubbins, K. E. *Theory of Molecular Fluids*, Vol. 1; Clarendon: Oxford, U.K., 1984.

Table 1

The values of LJ potential parameters and point charges applied in simulations

Molecule	Geometric parameters	Centre	σ [nm]	ε/k_B [K]	q/e	Reference
CO_2	$l_{C=O}$ = 0.1162 nm	C	0.2824	28.680	+ 0.664	93
		O	0.3026	82.000	– 0.332	
CH_4	l_{C-H} = 0.1090 nm	C	0.3400	55.055	– 0.660	89
		H	0.2650	7.901	+ 0.165	
		C-H[a)]	0.3025	30.600	–	
VPC	$l_{C=O}$ = 0.1233 nm	C[b)]	0.3400	28.000	–	59
		C[c)]	0.3400	28.000	+ 0.500	
		O	0.2960	105.800	– 0.500	

[a)] cross-interaction parameters

[b)] non-carbonyl group atom of C

[c)] carbonyl group C atom
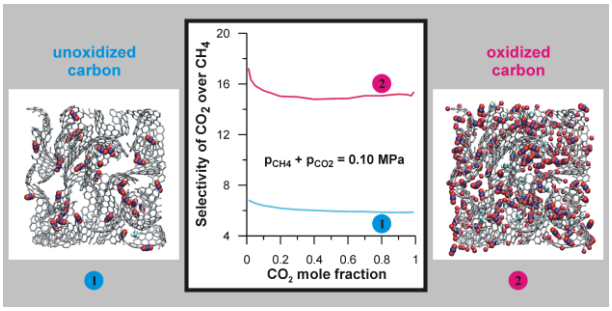
TABLE OF CONTENTS (TOC)